Progress in Scanning Electrochemical Microscopy by Coupling Potentiometric and Amperometric Measurement Modes

R. M. Souto[1], J. Izquierdo[1], J. J. Santana[1,2], A. Kiss[3], L. Nagy[3] and G. Nagy[3]

[1] Department of Physical Chemistry, Faculty of Chemistry, University of La Laguna, E-38200 La Laguna (Tenerife), Spain
[2] Department of Process Engineering, University of Las Palmas de Gran Canaria, E-35017 Las Palmas de Gran Canaria, Canary Islands, Spain
[3] Department of General and Physical Chemistry, Faculty of Sciences, University of Pécs, 7624 Pécs, Ifjúság útja 6, Hungary

Abstract:

Scanning electrochemical microscopy (SECM) with coupled potentiometric and amperometric measurement modes is used to study corrosion reactions in aqueous environments. Whereas conventional electrochemical techniques lack spatial resolution and provide little information on behaviour at sites of corrosion initiation or at defects, the advent of scanning electrochemical microscopy is contributing to overcome these limitations when applied to the investigation of corrosion processes *in situ*. Ion-selective microelectrodes (ISME) and dual amperometric/potentiometric probes have been developed that can be employed as SECM tips as they exhibit sufficiently low resistances and response times. The applicability of this experimental approach is demonstrated by chemically imaging the behaviour of an iron-magnesium galvanic couple immersed in a diluted aqueous electrolyte. The dissolution of metal ions from anodic sites, the consumption of oxygen at the cathodic sites, and the local pH changes associated with both half cell reactions are thus effectively monitored.

Keywords: Scanning electrochemical microscopy; corrosion; potentiometric detection; ion selective electrodes.

1. Introduction

Microelectrodes positioned in the vicinity of a sample can be employed as probes in scanning microscopies to achieve chemical sensitivity. The probe is moved parallel to the sample's surface inside an electrochemical cell and changes in the probe response are related to local chemical reactivity. Local variations of the substrate potentials are the measuring principle in the Scanning Reference Electrode Technique (SRET) [1], whereas technical developments either employ a vibrating probe for enhanced resolution of ionic current fluxes in the electrolytic phase (Scanning Vibrating Electrode Technique, SVET) [2], or introduce ion-selective microelectrodes for the monitoring of concentration changes related to surface dynamics (Scanning Ion-selective Electrode Technique, SIET) [3]. These techniques can measure changes related to either membrane-transport processes in biological systems [4], or ionic-transport processes in corrosion reactions [5]. It must be noticed that these methods are not able to modify any surfaces, and they exclusively monitor chemical heterogeneities at the sample's surface related to on-going chemical processes.

A different approach involved the introduction of microelectrodes to scanning probe microscopies, particularly modifying the scanning tunnelling microscope (STM) to monitor the electrochemical reactivity of a metal/electrolyte interface leading to the development of the scanning electrochemical microscopy (SECM) [6]. Conversely to other electrochemical scanning probe techniques, SECM needs a redox mediator in solution. That is, a reaction occurring at the microelectrode tip with an active species in the liquid electrolyte is the measuring principle (i.e., amperometric operation). Under steady-state operation, changes in the faradaic current measured at the tip due to the proximity of the sample's surface can be related to local electrochemical properties of the sample and to the distance towards the tip [7]. Since SECM operation requires chemical changes in redox species to occur due to the tip operation, it can be employed to modify surfaces or inside surface films by delivering electrolytically generated reagents to different locations in a controlled time [8].

Despite the major success of SECM operated amperometrically to monitor corrosion reactions [9,10], based on the conversion of the M^{z+} ions released at the anodic sites [11,12], or the depletion of oxygen content in the solution volume adjacent to the cathodic sites [13], there are still some relevant systems in corrosion science that cannot be investigated by this technique. Namely, in certain corroding samples, especially for metals with sufficiently negative redox potentials in aqueous environments, the use of noble metal microelectrodes is limited by the onset of oxygen reduction and hydrogen evolution reactions. On the other hand, Pt microelectrodes are not able to detect pH alterations, though the corrosion processes are dramatically affected by this parameter.

Furthermore, some metal ions may undergo hydrolysis at the anodic sites, and consequently reduce the pH, a feature that usually accelerates the corrosive attack. Though scarcely applied, these physicochemical parameters may be studied using ion-selective electrodes (ISME) as tips. In this case, the SECM should be operated in the potentiometric mode, which gives greater chemical selectivity for sensing species generated at the substrate without their consumption [14]. The most usual potentiometric probes are ion-selective reference microelectrodes [15], and pH microsensors [16]. Ion-selective micropipette electrodes are widely employed in experimental life sciences [17]. They are also employed in SIET to investigate some corrosion systems [3]. Ion-selective electrodes can be fabricated using a well-established procedure [18], because they depend on the chosen "ionophore cocktail" for selectivity. However, three main drawbacks were encountered when they were considered for use in SECM, namely, the resistivity and the fragility of the probe, and its time-response [14]. A new opportunity has been offered by the recent development of ion selective micropipettes containing a solid internal contact [19]. Owing to this design, the resistances of these solid-contact micropipette electrodes are only fractions of the resistance of conventional micropipette electrodes of the same size, which have a liquid contact, and may offer improved SECM performance. Their advantageous performance was also probed *in vivo* in both plant and animal tissue experiments [20].

In this contribution, the potentiometric and amperometric operation modes of SECM will be briefly described, and selected applications in the investigation of corrosion reactions will be provided in order to illustrate the application of ion-selective and dual amperometric/potentiometric microelectrodes as SECM tips in sensing localised corrosion.

2. SECM operation

The SECM instrument basically consists of a combination of electrochemical components, positioners and computer control. Figure 1A shows a schematic diagram of the basic SECM instrument employing an amperometric microprobe. The SECM is a technique in which a faradaic current flows through a microelectrode immersed in an electrolytic solution and situated close to a substrate. The microelectrode and the substrate form part of an electrochemical cell which is also constituted by reference and auxiliary electrodes, and sometimes by a second working electrode. The electrochemical setup is constituted by this electrochemical cell together with the bipotentiostat, which is the actual electrochemical interface. It allows the potential of the microelectrode and/or the substrate versus the reference electrode to be controlled, as well as to measure the current flowing between any of the working electrodes and the counter electrode. The microelectrode is a microdisc electrode, in which the electrode material is surrounded by an insulating shield. The most common

procedure for its fabrication is the encapsulation of the electrode material (carbon fibers or noble metal wires) in glass capillaries and the subsequent polishing of the tips to expose the microdisc surface. The microelectrode displacement and its position relative to the substrate are controlled with a three-dimensional microstage that provides independent and accurate control in the *x*-*y*-*z* axis. The remaining component is the data acquisition and display system, usually conformed by a computer, an interface and a display system. Details on the geometric characterization of the microelectrode tip, and on the operation procedures in amperometric SECM are given in ref. [10].

The same SECM instrument could be employed for the potentiometric measurements, though in this case a 10^{12} Ω input impedance operational amplifier was introduced in the measuring circuit as shown in Figure 1B. The cell voltage data were collected with a PC through the electrometer included in the electrochemical interface (Autolab potentiostat/galvanostat). The distance between the ISME and the substrate was established by allowing the probe to gently rest on the sample, using a video microscope to assist the process. Subsequently, the probe would be retracted to the chosen operation distance with the aid of the *z*-positioning motor.

3. Preparation and characterization of the micropipette ion-selective electrodes

The ionophore cocktail used in the construction of the Mg^{2+}-selective microelectrode was composed by tetrahydrofurane (THF) as solvent, poly(vinyl chloride) (PVC), bis-N,N-dicyclohexyl-malonamide, potassium tetrakis(4-chlorophenyl)borate (PTCB), and 2-nitrophenyl octyl ether (oNPOE). The optimum ratios of these components were established using the methodology described elsewhere [18,21], and the composition of the mixture required for the fabrication of 500 μm thick membranes [22] is given in Table 1.

3.1 Preparation of the micropipette ion-selective electrode

The micropipettes of desired size were built from borosilicate glass capillaries, previously soaked in “piranha” solution and thoroughly washed with twice deionized water. The ionophore cocktail was then introduced in the micropipette under suction. A carbon fiber was employed to ensure the internal contact with the cocktail, whereas the other end of the fiber was soldered to a copper wire to produce the electrical connection between the ISME and the external equipment. The portion of the carbon fiber to be inserted in the cocktail was previously coated with the conductive polymer PEDOT in an electrochemical cell composed by the carbon fiber as working electrode, an Ag/AgCl wire immersed in the electrolyte as reference electrode, and a Pt wire as the auxiliary electrode. The monomer employed was 3,4-ethylenedioxythiophene dissolved in $BMIM^+$ PF_6^- ionic liquid [22].

Finally, Loctite® adhesive was used to seal the rear of the ISME. A micrograph of the tip of this solid contact micropipette electrode is shown in Figure 2A.

3.2 Electropolymerization of the carbon fiber

The carbon fiber was electrochemically coated by PEDOT prior to insertion in the ionophore cocktail in order to ensure good electrical contact. The electropolymerization process was performed by subjecting the coated carbon fiber to ten potential cycles between -0.90 and +1.30 V vs. Ag/AgCl pseudo-reference. Potential cycling was performed at a sweep rate of 0.05 V/s, and Figure 2B depicts the current-potential response of the system recorded during this process. Subsequently, the cell electrolyte was replaced by $BMIM^+$ PF_6^- ionic liquid free from EDOT, and doping of the polymer film on the carbon fiber was done by potential cycling from -0.90 to +0.80 V vs. Ag/AgCl pseudo-reference. Five potential cycles with 0.05 V/s scanning rate were completed at this stage as shown in Figure 2C. The stability of the working electrode immersed in 0.1 M KCl was checked by recording five cyclic voltammograms (CV) scanning between -0.40 and +0.50 V vs. Ag/AgCl pseudo-reference (see Figure 2D).

The micropipette electrode was silanized using 5% dimethyldichlorosilane in heptane. This process was conducted by inserting a few μL of silinizing solution inside the tip of the pipette and then kept in 80^{o}C oven for 30 min. Next, the membrane cocktail was introduced into the tip of this pipette by using a very thin glass capillary attached onto the end of a syringe needle to produce back filling. The solid contact micropipette preparation was completed by placing the thinner pipette inside its lumen trying to position the carbon fiber inside the cocktail close to the orifice of the tip.

3.3 Calibration of the Mg^{2+}-ion selective microelectrode

We were primarily involved in producing a membrane cocktail that would show good selectivity and resolution towards monitoring the activity Mg^{2+} dissolved ions in aqueous environments as result of corrosion reactions from either magnesium-based or magnesium-containing alloy materials. A silver chlorinated wire was inserted into the internal solution as the inner reference electrode. The open circuit potential of the resulting sensor with respect to an external reference electrode arises from the potential difference between both sides of the membrane, which depends on the activity of the electrolyte in the tested solution with linear Nernstian response following equation (1):

$$E = E_0 + \frac{RT}{nF}\ln\left(a_{M^{n+}}\right) \qquad (1)$$

were $a_{M^{n+}}$ is the activity of the ion to be detected. The concentration range with linear Nernstian response will be conditioned by the composition of the ionophore cocktail, that includes other

compounds such as solvents, plasticizers or polymer resin, in order to improve the mechanical properties and selectivity against other ions.

The Mg^{2+}-ISME was calibrated using 1 mM NaCl as base electrolyte, with standard solutions of $MgCl_2$ of concentrations 10^{-1} to 10^{-5} M as shown in Figure 3A. The ISME was washed between different measurements. A linear response was found in Figure 3B for the range $1 \leq pMg \leq 3$. The observed (25.6 mV/decade) is sufficiently close to the expected Nernstian value of 29.6 mV/decade as to employ this electrode for quantitative measurements.

4. Preparation and characterization of dual amperometric/potentiometric electrodes

Electrodes made of antimony and coated by the metal oxide have the ability to behave as a double function electrodes. That is, they can be used as amperometric SECM tip for the measurement of faradaic currents when antimony is in the metallic state, whereas its oxidized state allows pH monitoring [16].

4.1 Preparation of the antimony electrode

Using a gas flame, melted antimony from metal powder is introduced in a Pyrex glass capillary under suction. Antimony-filled fibers are then fabricated using a pipette puller system, and they are introduced in the lumen of a micropipette with the tip reaching out for about 15 mm. Electric contact is ensured by inserting liquid mercury metal and a copper wire in the lumen of the micropipette. Loctite® adhesive was used to seal the two micropipette ends. Disk-shaped tips are thus obtained, with an active antimony electrode at the centre, surrounded by glass. Figure 4A shows a micrograph of the antimony microelectrode tip.

4.2 Characterization of the antimony microelectrode for amperometric operation

Geometric characteristics greatly determine the amperometric operation of a disk-shaped tip in amperometric SECM. The dimensions of the active metal surface, and the effect of the insulating glass shield, can be characterized by CV. A simple redox reaction is employed for this end. Figure 4A shows a CV of the electrode immersed in naturally aerated 1 mM NaCl solution, giving an almost diffusive behavior for oxygen reduction at potentials between -0.60 and -0.80 V vs. Ag/AgCl/KCl (3M), as depicted in the inset. Analogously, the CV of the electrode in a deoxygenated $[Ru(NH_3)_6]Cl_3$ solution is presented in Figure 6B, showing a reduction peak at around -0.20 V vs. Ag/AgCl/KCl (3M). Though this is not exactly the typical behavior presented by microelectrodes, it still can be considered in the limit between macroscopic- and microscopic-sized electrodes because it

exhibits a nearly diffusive response. The electrochemical data are consistent with the dimensions of an antimony disk electrode with dia. 175 μm, and RG = 2.9.

4.3 Calibration of the antimony microelectrode as pH sensor

Antimony microelectrodes were calibrated by measuring their open circuit potentials in nine buffer solutions. The typical calibration procedure was performed by introducing the microelectrode in a sequence of buffer solutions initiated with the most alkaline solution. In this way, the tip was exposed to solutions of increased acidity as shown in Figure 5A**.** The overpotential values observed in the plot occurred upon electrolyte exchange, and next the electrode attained a steady potential value in each solution. With the potential values taken from each buffer solution, the calibration plot shown in Figure 5B was drawn. It can be observed that there is a linear relationship between the potential of the antimony tip and the solution pH in the interval between 4 and 11. The slope of the plot amounts to 42.3 mV/pH unit. Though this value is not fully Nernstian, this behavior has been observed before [23].

5. Experimental investigation of galvanic corrosion

Galvanic corrosion can occur when two dissimilar metallic materials are in electrical contact with each other for electron transfer and are exposed to an electrolytic environment. A material with a lower free corrosion potential in a galvanic couple becomes more active and corrodes preferentially. The corrosion rate of a galvanic couple in electric or direct contact is a technological challenge which can only be estimated with conventional electrochemical techniques. In this context, spatially-resolved chemically-sensitive microelectrochemical techniques may open a new route for quantitative characterization of those systems. In this work, we have selected a model galvanic couple as a test system for the applicability of highly selective tips in scanning electrochemical microscopy for corrosion research.

Magnesium-steel galvanic pairs can be encountered in aerospace and automobile applications, thus providing a corrosion problem of technological interest. For the sake of simplicity, iron could be considered instead of steel at this preliminary stage. The galvanic Fe-Mg couple employed for this study consisted on one sheet of magnesium and either a wire or a strip of iron immobilized in *Epofix*® resin. Both metals were fixed vertically in the resin, facing up their rectangle cross sections as the active surfaces to be analyzed. The separation between the two metals was ca. 5 mm. The resulting mount containing the embedded metals had a circular top surface of 3 cm diameter. The surface of the specimen was wrapped around laterally by sellotape. Thus a small container for about

5 ml of electrolyte was created for use in the microelectrochemical measurements. The test electrolyte was 1 mM NaCl aqueous solution.

SECM experiments consisted in recording the distribution of concentrations for the chemical species involved in the galvanic corrosion process. The mount containing the two metals was scanned with the relevant SECM tips in close proximity to the surface, thus allowing chemical activity to be mapped. Initially, the two metals were left without electric contact between them, thus actually attaining their corresponding open circuit potentials in the test electrolyte. After recording the relevant SECM images over the insulated metals, the galvanic coupling effect was subsequently achieved by connecting the two metals at the rear of the mould.

The ability of the ISME to respond to changes in the concentration of magnesium soluble species as result of the onset of corrosion reactions, was first investigated using the magnesium strip as a source of its ions. In this case, the ISME tip of the SECM was placed just above the centre of the magnesium sample, and its potential was monitored with the elapse of time. A steady reading was obtained as long as the metal was maintained without galvanic coupling with iron. After a selected time, galvanic coupling of the metals was imposed, and enhanced dissolution of magnesium occurred as result of it. This resulted in potential oscillations in the recording of the tip as shown in Figure 6 which depicts the behaviour in the case of two such experiments. Less negative values of the potential at the ISME are observed because a higher amount of magnesium ions have been released into the solution from the metal surface. Vigorous hydrogen gas evolution over the magnesium strip was also observed through the videocamera. It has been demonstrated that the tip responds to variations in the activity of magnesium ions due to an increase in the rate of corrosion of the metal.

Figure 7 shows the SECM maps related to the spatial distribution of magnesium ions that were recorded using the solid contact Mg^{2+}-ISME. In the case of the uncoupled metal (cf. Figure 7A), active corrosion of the magnesium strip is observed to occur in this electrolyte, leading to the release of metal ions into the solution. Nevertheless, the anodic activity is observed to concentrate on a portion of the metal strip (located in the upper part of the image). Thus, the remaining surface of the metal actually acts as a cathode to maintain the corrosion process, as indicated by the pMg values close to zero that are measured in the lower part of the exposed sample. Upon galvanic coupling of the two metals, enhanced dissolution of the magnesium strip occurs, resulting in pMg values almost three orders of magnitude greater than those recorded for the uncoupled metal. Furthermore, the metal dissolution process now extends over all the length of the exposed metal strip, though the process occurs heterogeneously, with anodes shifting positions over the exposed metal (see Figure 7B).

Changes in the solution pH close to the mount, which are associated with the corrosion process, could be monitored when the antimony microelectrode was employed for the potentiometric operation of the SECM. Figure 8 depicts the pH distributions occurring over the magnesium strip for the uncoupled (image A) and the coupled (image B) metal. For the uncoupled metal, alkalinization of the electrolyte volume close to the surface occurs. In this case, an almost homogeneous distribution of pH is found over the metal, whereas the pH decreases as the tip scans about the epoxy mount surrounding the metal strip. Conversely, upon galvanic coupling, the magnesium surface becomes less alkaline, because the cathodic activity is now moved to the iron wire (image C). Yet, the pH distribution above the magnesium strip is heterogeneous, and the less alkaline areas correspond to sites where dissolution occurs preferentially.

Finally, the antimony tip could also be employed to monitor the corresponding cathodic process by measuring oxygen consumption with the SECM in amperometric operation. The images given in Figure 9 show the regions with depleted oxygen in the electrolyte adjacent to the iron strip, as those where the tip recorded smaller faradaic currents [10]. Again, a major change is observed in the SECM images when the two metals are coupled, as illustrated by the higher peak in Figure 9B. In this case, tip currents close to 0 nA were measured over the metal, thus showing that oxygen was absent from the thin electrolyte volume comprised between the tip and the iron strip. This proves that the whole metal was behaving as a cathode when galvanically-coupled to magnesium. Therefore, the iron strip is effectively protected from corrosion through its connection with the sacrificial anode of magnesium.

6. Concluding remarks

Significant improvement in SECM for the investigation of corrosion processes is achieved by combining amperometric and potentiometric operations in the instrument. Dual amperometric/potentiometric tips based on the special properties of certain oxides of transition metals such as antimony allow conventional SECM operation and pH detection in the same experiment. Furthermore, ion-selective microelectrodes based on micropipettes with an internal solid contact, are robust enough to be employed as SECM tips for selective detection of relevant chemical species. Thus, combinations of operation modes in SECM can be employed for more sensitive applications of SECM imaging in corrosion science.

Acknowledgements The authors are grateful to the Spanish Ministry of Science and Innovation (MICINN, Madrid, Acción Integrada No. HH2008-0011) and to the National Office for Research and Technology (NKTH, Budapest, research grant ES-25/2008 TeT) for the grant of a Collaborative Research Programme between Hungary and Spain. J.J.S., J.I., and R.M.S. are grateful for financial

support by the MICINN and the European Regional Development Fund (Brussels, Belgium) under Projects No. CTQ2009-12459 and CTQ2009-14322. A Research Training Grant awarded to J.I. by the Spanish Ministry of Education (MECD, Madrid, *Programa de Formación de Personal Investigador*) is gratefully acknowledged. L.N., G.N., and A.K. acknowledge support from "Developing Competitiveness of Universities in the South Transdanubian Region (SROP-4.2.1.B-10/2/KONV-2010-0002)".

References

[1] Lillard RS. Scanning electrode techniques for investigating near-surface solution current densities. In: Marcus P, Mansfeld F, eds. *Analytical methods in Corrosion Science and Engineering.* Boca Raton: Taylor and Francis; 2006:571-604.

[2] Jaffe LF, Nuccitelli R. An ultrasensitive vibrating probe for measuring steady extracellular currents. *Journal of Cell Biology.* 1974;63:614-628.

[3] Lamaka SV, Souto RM, Ferreira MGS. In-situ visualization of local corrosion by Scanning Ion-selective Electrode Technique (SIET). In: Méndez-Vilas A, Díaz J, eds. *Microscopy: Science, Technology, Applications and Education. Vol. 3.* Badajoz: Formatex; 2010:2162-2173.

[4] Smith PJS, Sanger RH, Messerli MA. Principles, development and applications of self-referencing electrochemical microelectrodes to the determination of fluxes at cell membranes. In: Michael AC, Borland LM, eds. *Electrochemical methods for neuroscience*. Boca Raton: CRC; 2007:373–405.

[5] Rossi S, Fedel M, Deflorian F, Vadillo MC. Localized electrochemical techniques: Theory and practical examples in corrosion studies. *Comptes Rendue Chimie.* 2008;11:984-994.

[6] Bard AJ, Fan F-RF, Kwak J, Lev O. Scanning electrochemical microscopy. Introduction and principles. *Analytical Chemistry*. 1989;61:132-138.

[7] Kwak J, Bard AJ. Scanning electrochemical microscopy - Theory of the feedback mode. *Analytical Chemistry*. 1989;61:1221-1227.

[8] Bard AJ, Denuault G, Lee C, Mandler D, Wipf DO. Scanning electrochemical microscopy - A new technique for the characterization and modification of surfaces. *Accounts of Chemical Research*. 1990;23:357-363.

[9] Niu L, Yin Y, Guo W, Lu M, Qin R, Chen S. Application of scanning electrochemical microscope in the study of corrosion of metals. *Journal of Materials Science*. 2009;44:4511-4521.

[10] Souto RM, Lamaka SV, González S. Uses of scanning electrochemical microscopy in corrosion research. In: Méndez-Vilas A, Díaz J, eds. *Microscopy: Science, Technology, Applications and Education. Vol. 3.* Badajoz: Formatex; 2010:1769-1780.

[11] González-García Y, Burstein GT, González S, Souto RM. Imaging metastable pits on austenitic stainless steel in situ at the open-circuit corrosion potential. *Electrochemistry Communications.* 2004;6:637-642.

[12] Souto RM, González-García Y, González S. In situ monitoring of electroactive species by using the scanning electrochemical microscope. application to the investigation of degradation processes at defective coated metals. *Corrosion Science.* 2005;47:3312-3323.

[13] González S, Santana JJ, González-García Y, Fernández-Mérida L, Souto RM. Scanning electrochemical microscopy for the investigation of localized degradation processes in coated metals: Effect of oxygen. *Corrosion Science.* 2011;53:1910-1915.

[14] Denuault G, Nagy G, Tóth K. Potentiometric probes. In: Bard AJ, Mirkin MV, eds. *Scanning electrochemical microscopy*. New York: Marcel Dekker; 2001:397-444.

[15] Nagy G, Nagy L. Electrochemical sensors developed for gathering microscale chemical information. *Analytical Letters*. 2007;40:3–38.

[16]Horrocks BR, Mirkin MV, Pierce DT, Bard AJ, Nagy G, Tóth K. Scanning electrochemical microscopy. 19. Ion selective potentiometric microscopy. *Analytical Chemistry.* 1993;65:1213–1224.
[17]Messerli MA, Collis LP, Smith PJS. Ion trapping with fast-response ion-selective microelectrodes enhances detection of extracellular ion channel gradients. *Biophysics Journal.* 1999;96:1597-1605.
[18]Craggs A, Moody GJ, Thomas JDR. PVC matrix membrane ion-selective electrodes. Construction and laboratory experiments. *Journal of Chemical Education.* 1974;51:541-544.
[19]Gyetvai G, Sundblom S, Nagy L, Ivaska A, Nagy G. Solid contact micropipette ion selective electrode for potentiometric SECM. *Electroanalysis.* 2007;19:1116-1122.
[20]Gyetvai G, Nagy L, Ivaska A, Hernadi I, Nagy G. Solid contact micropipette ion selective electrode II: Potassium electrode for SECM and in vivo applications. *Electroanalysis.* 2009;21:1970-1976.
[21]Lindner E, Gyurcsányi RE, Back RP. Tailored transport through ion-selective membranes for improved detection limits and selectivity coefficients. *Electroanalysis.* 1999;11:695-702.
[22]Bodor S, Zook JM, Lindner E, Tóth K, Gyurcsányi RE. Electrochemical methods for the determination of the diffusion coefficient of ionophores and ionophore–ion complexes in plasticized PVC membranes. *Analyst*. 2008;133:635–642.
[23]Izquierdo J, Nagy L, Varga Á, Santana JJ, Nagy G, Souto RM. Spatially-resolved measurement of electrochemical activity and pH distributions in corrosion processes by scanning electrochemical microscopy using antimony microelectrode tips. *Electrochimica Acta.* 2011;56:8846-8850.

Table 1 Composition of the mixture employed to produce the ionophore cocktail for the Mg^{2+} ion-selective microelectrodes

Component	Quantities for 200 µL of the mixture	
	Content	wt.%
Tetrahydrofurane (THF)	100 µL	-
Poly(vinyl chloride) (PVC)	7.68 mg	5.06
bis-N,N-dicyclohexyl-malonamide	2.23 mg	1.47
Potassium tetrakis(4-chlorophenyl)borate (PTCB)	2.13 mg	1.40
2-nitrophenyl octyl ether (oNPOE)	139.79 mg	92.07

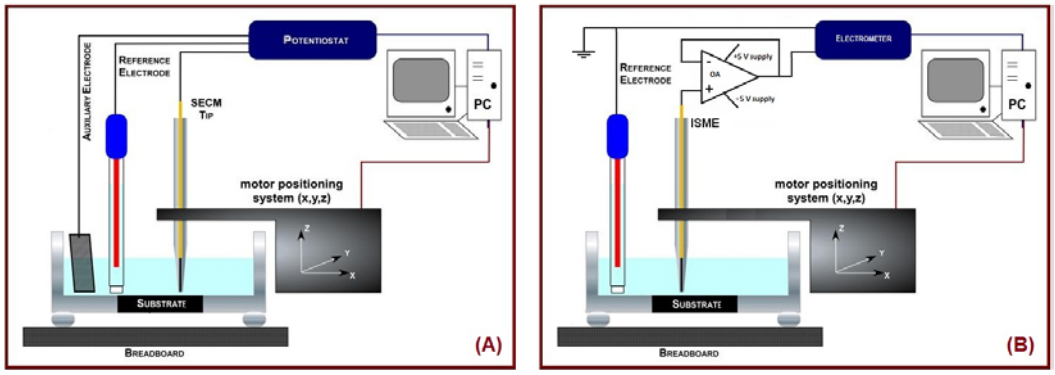

Fig. 1 Sketches showing the main components of the instruments employed for (A) amperometric, and (B) potentiometric SECM measurements, including the high input impedance operational amplifier (OA), and the ion-selective electrode (ISME).

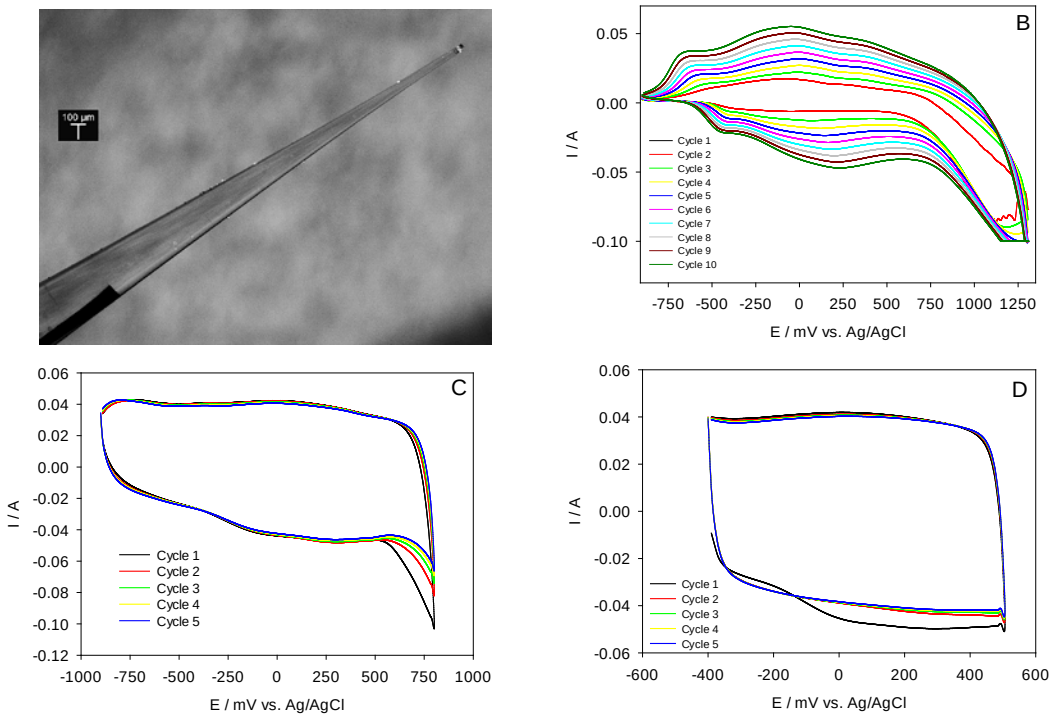

Fig. 2 (A) Micrograph of the solid contact Mg^{2+}-ISME. (B-D) Cyclic voltammograms recorded during the preparation of the solid contact micropipette ISME. The goal and the electrolyte of the three steps described in the figure are, respectively: (B) coating of the carbon fiber by polymerization, with 3,4-ethylenedioxythiophene dissolved in $BMIM^+$ PF_6^- ionic liquid; (C) doping, in $BMIM^+$ PF_6^- ionic liquid free of the monomer; and (D) testing, in 0.1 M KCl. v = 0.05 V/s.

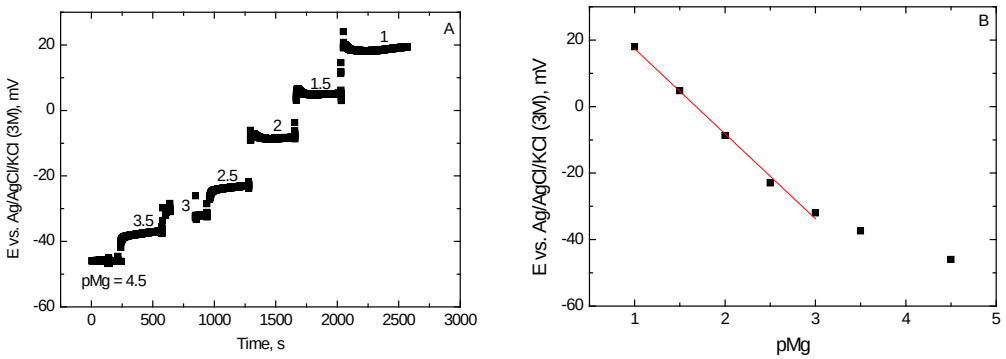

Fig. 3 (A) Transient response and, (B) resulting calibration plot for the Mg^{2+} ion selective micropipette electrode in 1 mM NaCl solutions containing varying amounts of $MgCl_2$ ($pMg = -\log_{10}[Mg^{2+}]$).

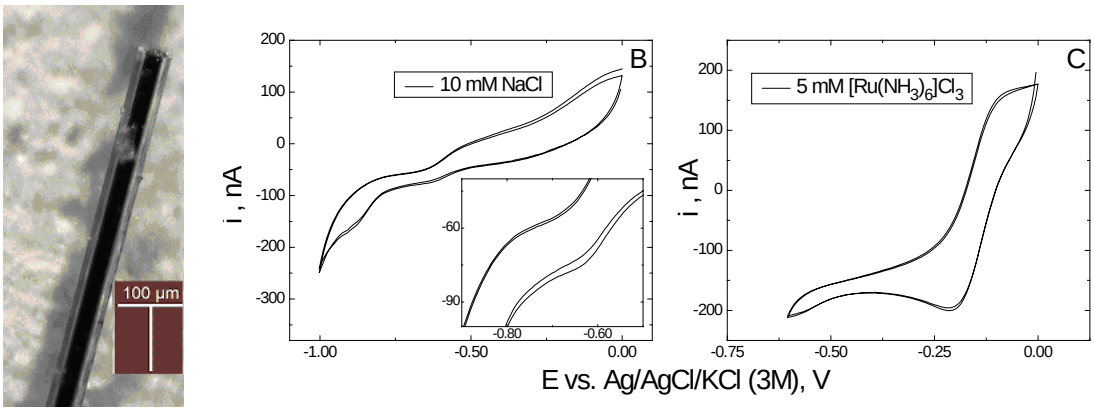

Fig. 4 (A) Micrograph of the antimony microelectrode. (B-C) Cyclic voltammograms recorded at this electrode in: (B) aerated 1 mM NaCl solution, and (C) deaerated 5 mM $[Ru(NH_3)_6]Cl_3$ + 0.1 M NaCl solution. v = 0.01 V/s. Tip parameters: a = 87 µm, RG = 2.9.

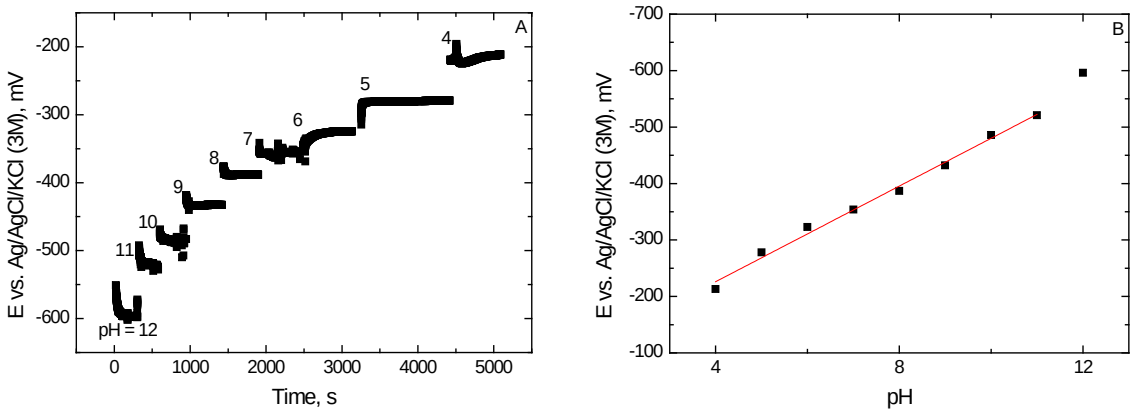

Fig. 5 (A) Transient response, and (B) corresponding calibration plot for the antimony electrode in buffered pH solutions.

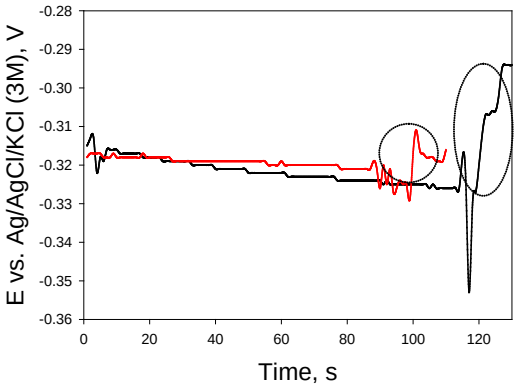

Fig. 6 Potentiometric SECM measurement of the potential variation with time occurring at a solid contact Mg^{2+}-ISME placed just above the magnesium strip in an iron-magnesium galvanic pair immersed in 10 mM NaCl. The two wires were maintained electrically-disconnected until connected for the times indicated by the circles in the plot.

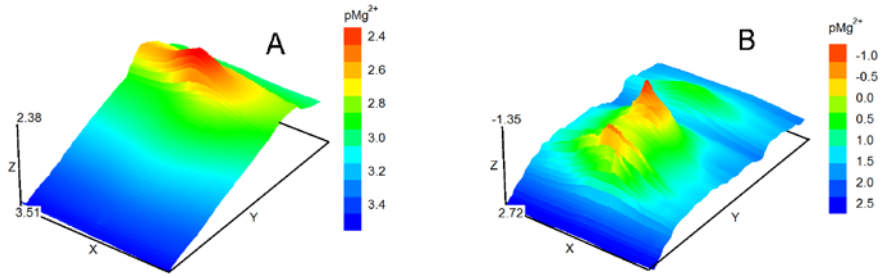

Fig. 7 Potentiometric SECM images measured with the Mg^{2+}-ISME depicting the magnesium ion concentration over the magnesium strip when the iron-magnesium sample was immersed in 1 mM NaCl. The metals were: (A) without, and (B) with galvanic connection. The figures represent an area of 1000 µm x 1500 µm in *X* and *Y* directions, respectively.

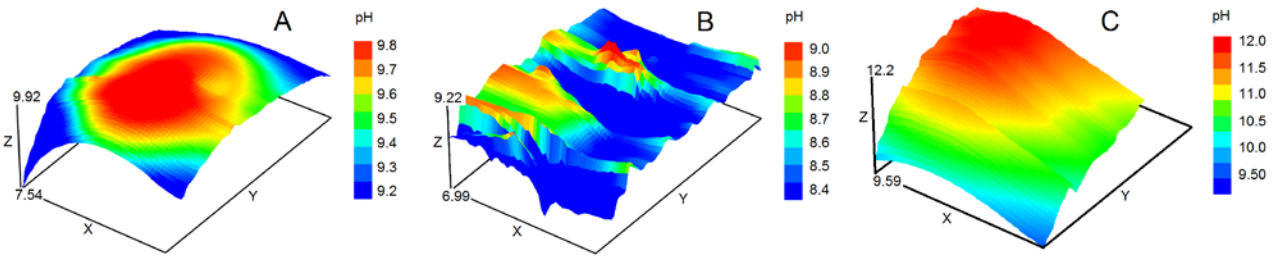

Fig. 8 Potentiometric SECM images measured with the antimony electrode depicting pH distribution over the magnesium strip and iron wire when the iron-magnesium sample was immersed in 1 mM NaCl. The metals and electrical conditioning were: (A) uncoupled magnesium, (B) galvanically-coupled magnesium, and (C) galvanically-coupled iron. The figures represent an area of: (A,B) 1000 µm x 1500 µm, and (C) 1500 µm x 1500 µm in *X* and *Y* directions, respectively.

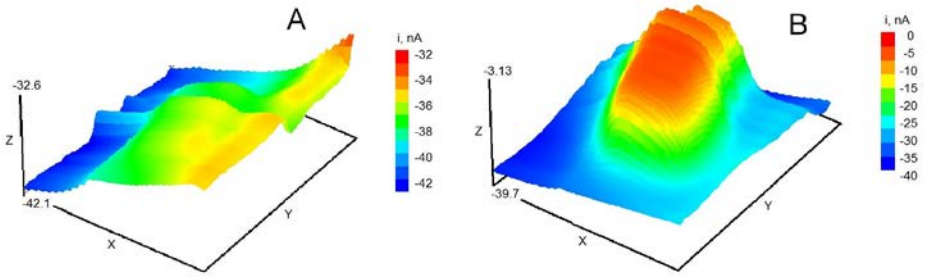

Fig. 9 Amperometric SECM images measured with the antimony tip depicting oxygen consumption over the iron strip when the iron-magnesium sample was immersed in 10 mM NaCl. The metals were: (A) without, and (B) with galvanic connection. Tip potential: -0.70 V vs. Ag/AgCl/KCl (3M). The figures represent an area of 2500 μm x 3000 μm in *X* and *Y* directions, respectively.